

16<sup>th</sup> Australasian Fluid Mechanics Conference  
Crown Plaza, Gold Coast, Australia  
2-7 December 2007

## Factors Affecting Grid-independent Results for Compartment Fire Modelling

K.A.M. Moinuddin and I.R. Thomas

Centre for Environmental Safety and Risk Engineering,  
Victoria University, P.O. Box 14428, MCMC, Victoria, 8001 AUSTRALIA

### Abstract

Obtaining grid independent results for compartment fires using a computational fluid dynamics (CFD) model is a major challenge, especially when the fire is not prescribed. While simulating a fire scenario using a CFD model, most fire safety engineers use computational cell sizes that can only be supported by their computing resources which may lead to a large error. This paper presents a systematic study to obtain a grid independent result from CFD simulations of an ISO 9705 room fire experiment using the CFD package Fire Dynamics Simulator (FDS) which incorporates a large eddy simulation (LES) methodology along with a mixture fraction combustion model. The experiment involved ignition of two trays of liquid fuel placed in the room and the growth and development of this fire. The study shows that initially as the grid sizes decrease the size of the fire increases and then the fire size starts decreasing to an asymptotic value as the grid sizes decrease further. A discussion is presented on the factors in relation to “goodness” of the grid resolution such as the changing trend of characteristic fire diameters, the size of computational cells etc.

### Introduction

To evaluate the performance of fire safety design, fire modelling is a highly desirable tool due to the high cost of experimental studies. In the current era of computing, the use of CFD is possible for real life fire scenarios. The FDS, developed at the National Institute of Standards and Technology (NIST), US [1], is such a CFD model. The FDS has been widely adopted by fire engineers due to some of its unique features (the ability to predict the course of a fire through ignition, growth, established burning and decline through to extinguishment or burnout). This model incorporates a simplified pyrolysis model, LES turbulence model, mixture-fraction combustion model, and finite-volume radiative heat transfer model.

In conducting CFD analysis it is essential to undertake a grid refinement process by gradually reducing the grid spacing (cell size) used in the analysis to examine the effect of the reduced cell size on the predicted outcome. It is usual to find that as the cell size is reduced the results converge. Thus further reducing the cell size has virtually no effect on the results produced and the result is known as grid-independent result. To be meaningful, any results obtained using a CFD fire model must be grid independent. In this study, a set of ISO 9705 room fires is chosen as several FDS validation studies were conducted by various research teams on this particular fire scenario as a representative of compartment fires. The objective of this particular study is to evaluate the size of the computational cells required to obtain grid independent results. From the numerical data an analysis of results will also be carried out to quantify the changing trend of heat release rate (HRR) with respect to computational cell sizes. This will provide fire safety engineers with useful numerical data and insight with which to judge their fire simulation results using computationally viable grids.

### Governing Equations

To model fire and smoke movement in LES methodology the large eddy motion is solved by a set of filtered equations governing the three-dimensional, time-dependent movements [2]. The filtered and simplified continuity, momentum and state equations for a low Mach number (<0.3) compressible flow that are solved in FDS are given below:

$$\frac{\partial \bar{\rho}}{\partial t} + \frac{\partial}{\partial x_i} (\bar{\rho} \bar{u}_i) = 0, \quad (1)$$

$$\bar{\rho} \left( \frac{\partial \bar{u}_i}{\partial t} + \bar{u}_j \frac{\partial \bar{u}_i}{\partial x_j} \right) = - \frac{\partial (\bar{p} - \bar{p}_o)}{\partial x_i} + \frac{\partial}{\partial x_j} \left\{ \mu \left( \frac{\partial \bar{u}_i}{\partial x_j} + \frac{\partial \bar{u}_j}{\partial x_i} \right) \right\} + \bar{\rho} g \delta_{i3} - \frac{\partial \tau_{ij}}{\partial x_j}, \quad (2)$$

$$\bar{p}_o = \bar{\rho} R \bar{T} \quad (3)$$

Density, velocity and temperature are solved by the continuity (Eq.1), momentum (Eq.2) and state (Eq.3) equations respectively. The divergence of the momentum equation yields a Poisson equation for the pressure. The basis of the simplification of the equations is to assume (a) that the speed of flow is much less than the speed of sound, (b) the temperature and density variation are large, and (c) the pressure variation is small. In these simplified equations, the pressure term in the equation of state and Poisson equation appears as  $\bar{p}_o$  which is the space-average pressure and independent of gas density.

In Eq. (2), the sub-grid Reynolds stresses are

$$\tau_{ij} = 2\bar{\rho}(\overline{u_i u_j} - \bar{u}_i \bar{u}_j)$$

which is modelled using the Smagorinsky model:

$$\tau_{ij} = 2\bar{\rho}(C_s)^2 \Delta^2 |\bar{S}| \bar{S}_{ij} \quad \text{where,}$$

$$|\bar{S}| = (2\bar{S}_{ij} \bar{S}_{ij})^{1/2}, \quad \bar{S}_{ij} = \frac{1}{2} \left( \frac{\partial \bar{u}_i}{\partial x_j} + \frac{\partial \bar{u}_j}{\partial x_i} \right),$$

with  $C_s$  value of 0.2.

As the combustion gas consists of a mixture of species (such as CO<sub>2</sub>, O<sub>2</sub> etc.), it is necessary to solve transport equations for each species. The species equation that is solved in this model is given as:

$$\frac{\partial \rho Y_i}{\partial t} + \nabla \cdot \rho Y_i \mathbf{u} = \nabla \cdot \rho D_i \nabla Y_i + \dot{W}_i''' \quad (4)$$

where  $Y_i$  is the mass fraction of the  $i$ th species,  $D_i$  is the diffusion coefficient of species  $i$  into the mixture,  $\mathbf{u}$  is the velocity vector ( $u_1, u_2, u_3$ ) and  $\dot{W}_i'''$  is the production rate of the species  $i$ .

Within the FDS mixture-fraction combustion model, since the reactants are not premixed, it is assumed that the reaction is diffusion controlled. Consequently the progress of the reaction would depend on the degree of mixing which is represented by the parameter defined as mixture-fraction  $Z$ . The mixture fraction satisfies the conservation law:

$$\bar{\rho} \frac{DZ}{Dt} = \nabla \cdot \bar{\rho} D \nabla Z \quad (5)$$

The assumption of infinite rate of reaction between fuel and oxygen together with Huggets relationship [3] for the HRR as a

function of oxygen consumption leads to the correlation:

$$\dot{q}_c'' = \Delta H_o \left. \frac{dY_o}{dz} \right|_{z=z_f} (\rho D) \nabla Z \cdot \mathbf{n} \quad (6)$$

where  $\dot{q}_c''$  is the rate of heat release per unit area of the flame sheet,  $Y_o$  is the oxygen mass fraction,  $D$  represents diffusivity,  $\mathbf{n}$  is the unit normal facing outward from the fuel and  $Z_f$  theoretical stoichiometric value [2].

It is postulated that by modifying the stoichiometric value it is possible to get a reasonable approximation of the HRR of the fire even when the fire is not well resolved. FDS includes such a routine as default. The program automatically reduces the stoichiometric value of the mixture fraction so that flame will shift away from its original position. This will in effect calculate larger flame height which will compensate for low resolution of fire. In FDS, the stoichiometric value of the main reaction is re-adjusted in accordance with the following relation:

$$\frac{Z_{f,eff}}{Z_f} = \min\left(1, C \frac{D^*}{\delta X}\right), \quad (7)$$

in which,  $D^*$  is the characteristic fire diameter,  $\delta X$  ( $=(\delta x \times \delta y \times \delta z)^{1/3}$ ) is the nominal grid cell size and  $C$  is an empirical constant with a value of 0.6. The relation between characteristic fire diameter and HRR is given by the equation:

$$D^* = \left( \frac{HRR}{\rho_\infty c_p T_\infty \sqrt{g}} \right)^{2/5} \quad (8).$$

$D^*/\delta X$  is a non-dimensional quantity whose value represents the number of computational cells spanning  $D^*$  and is considered representative of the “goodness” of the grid resolution. Previously, when a HRR, obtained from an ISO 9705 room corner fire experiment was prescribed into FDS [4], the grid independent gas temperature data at various locations was obtained with 50 mm cell i.e.  $D^*/\delta X \approx 10$  based on peak HRR. With this cell size, the experimental temperature data was found to be quite accurately predicted by the simulation. Zou and Chow [5] also obtained very good prediction of temperature and radiation data using  $D^*/\delta X$  of  $\approx 14$ , while the HRR was prescribed as obtained experimentally.

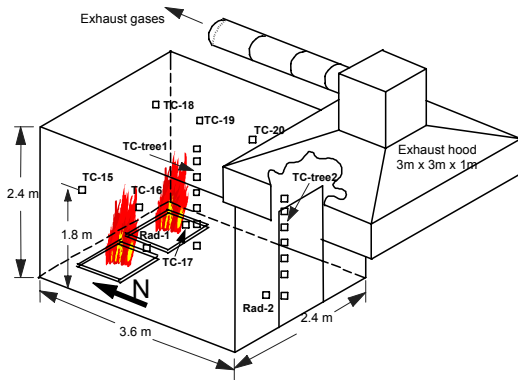


Figure 1. Schematic diagram of experimental set-up (fuel tray locations are shown for Back-Tray test).

### Brief Description of Experiment

Two tests (named as Back-Tray and Centre-Tray tests) which are simulated in this study were conducted at in the ISO room facility at Centre for Environmental Safety and Risk Engineering, Victoria University. Detailed room description is given in [6] which is also shown in Fig.1. The room was ventilated solely by a doorway 2.0 m high by 0.8 m wide (as specified in ISO 9705) located at the centre of one 2.4 m wall. The doorway was fully open during all of the tests. The outgoing products of combustion were collected by an exhaust hood and directed to an oxygen calorimeter [3].

Two fuel trays used were 0.81 m × 0.70 m by 0.05 m deep, 0.0032 mm thick and were constructed from steel. The trays were spaced 0.05 m and centrally placed 0.1 m and 1.4 m off the back wall for Back-Tray and Centre-Tray tests, respectively. Standard commercial grade methylated spirits, consisting of 97% ethanol and 3% water, was used as the fuel with 5 litres of fuel in each tray. The HRR versus time profiles from both tests are plotted in Fig.2.

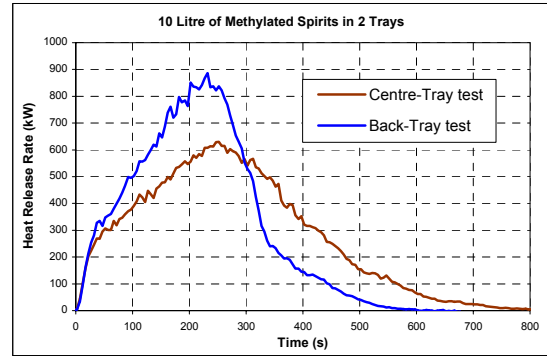


Figure 2. The HRR profiles obtained experimentally.

### Overview of FDS Simulation

#### Input data set-up

FDS data files were constructed to model the experimental set-up for the ISO room. The computational domain was extended beyond the enclosure to capture all of movement of air and combustion gases (Fig.3). However, in the lateral direction, half of the domain was modelled with the remainder represented using a SYMMETRY boundary condition as shown in Fig.3.

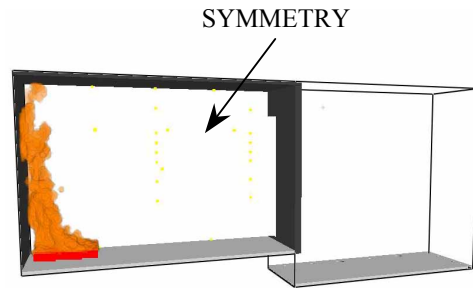


Figure 3. Computational domain of an ISO room fire.

The fuel-trays were modelled as an obstruction with dimensions similar to the actual size, placed appropriately in the room. The top face of the obstruction was used to simulate the fuel surface and the other faces were modelled as steel sheet. The limitation of this model is that it cannot take into account the container rim effect or heat transfer to the steel container; however no alternative is available for FDS version 4 (FDS4). The internal surfaces were modelled as a 0.0016 m steel sheet with a  $C\_DELTA\_RHO$  value of 6.4 and the backing specified as insulated. The floor was specified as 0.05 m concrete.

	Back-Tray (100 mm cell)		Centre-Tray (120 mm cell)	
	HRR (kW)	$D^*/\delta X$	HRR (kW)	$D^*/\delta X$
Peak	870	9	615	6.6
Average	355	6.3	278	3.8

Table 1.  $D^*/\delta X$  values corresponding to the experimental HRR values.

100 mm and 120 mm grid spacing for Back-Tray and Centre-Tray case simulations, respectively, corresponds to the  $D^*/\delta X$  values shown in Table 1. These values are calculated based on both peak and average HRR.

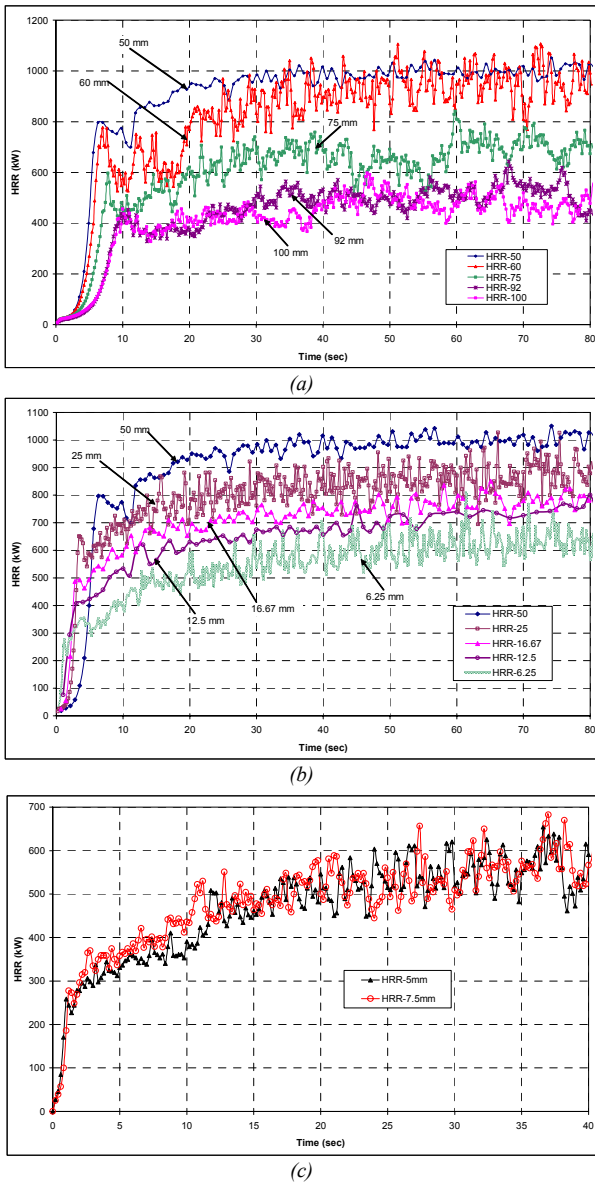


Figure 4. Predicted HRR profiles using different cell sizes (Back-Tray case).

For the Back-Tray case, simulations were conducted using nominal grid sizes ( $\delta X$ ) of 100, 92, 80, 75, 60, 50, 37.5, 25, 20, 16.67, 12.5, 9.375, 7.5, 6.25 and 5 mm. For the Centre-Tray case an additional simulation with 120 mm cell was conducted. However, no simulation was conducted with 7.5 and 5 mm cells, but will be conducted in future.

For simulations with cell sizes smaller than 50 mm, ‘multiple meshes’ were used so that regions containing flame were divided into the finer cell sizes mentioned above. Relatively coarse meshes were used in adjacent regions where no burning took place. Special care was taken to maintain virtually the same room size, shape and ventilation during all simulations as size can often vary as objects are ‘snapped’ to the grid. Special care was also taken to account for the variation of fuel surface area due to the same grid snapping issue. Most simulations were conducted using a PC with 3.2GHz Pentium processor and 2GB memory. However, simulations with a grid spaced less than 10 mm was conducted on a Linux based cluster system managed by Victorian Partnership of Advanced Computing (VPAC) due to the higher computational demand. During simulations FDS4 default options are used except the variations mentioned below.

**Combustion parameters and material properties**

The combustion parameters and material properties for the ethanol fuel and reaction used were from the FDS4 database except as follows. Firstly, the thermal properties of ethanol given were modified to allow for the effect of 3% water in the fuel. Secondly, based on [5], RADIATIVE\_FRACTION was set to 0.0, which means that the source term calculation in the radiation transport equation is based on the cell temperature rather than the heat released in the cell [1].

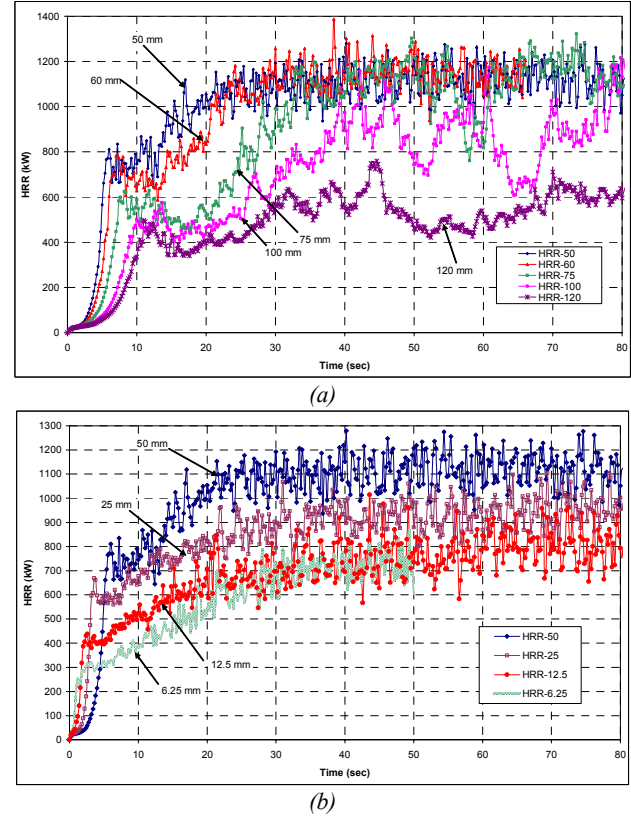


Figure 5. Predicted HRR profiles using different cell sizes (Centre-Tray case).

**Results and Discussion**

The HRR versus time profiles (Back-Tray case) up to 80 sec are plotted in Fig.4. The HRR values presented here are twice the values of computational results, as only half the domain was modelled as discussed. Fig.4(a) presents data from five simulations conducted using 100, 92, 75, 60 and 50 mm cells. It can be observed that as the cell size decreases the HRR increases. In Fig.4(b) data from seven simulations conducted using 50, 25, 16.67, 12.5 and 6.25 mm cells is shown. A phenomenon opposite to Fig.5(a) is observed i.e. as the cell size decreases the HRR also decreases. In Fig.5(c), HRR profiles from 7.5 and 5 mm cells are plotted up to 40 secs and it appears that grid convergence is occurring at 7.5 mm cells.

Similarly HRR versus time profiles of the Centre-Tray case are plotted in Fig.5. It is again found that as the grid size decreases initially, the size of the fire increases then begins to decrease as the grid size decreases further.

To quantify the changing trend of the HRR with respect to grid spacing, the HRR data presented in Figs. 4 and 5 have been time averaged for 65 seconds (approximately one-tenth of the experimental burnout time) and based on the averaged HRR using Eq.8  $D^*$  has been calculated. Fig.6 shows  $D^*$  from all simulations with respect to  $\delta X$ . Similar to Figs. 4 and 5, it can be seen that from a  $\delta X$  value of 0.1 m up to 0.05 m the value of  $D^*$

gradually increases and then the onward value of  $D^*$  gradually decreases leading to an asymptotic value. This asymptotic value could not be determined due to computational constraints, especially for the Centre-Tray case. However, using an Excel spreadsheet correlations (fourth order for Back-Tray and fifth order for Centre-Tray) leading to the asymptotic values (inferring grid independence) have been derived which is also plotted in Fig.6. The Centre-Tray correlation needs to be confirmed by conducting simulation with 7.5 and 5 mm cells.

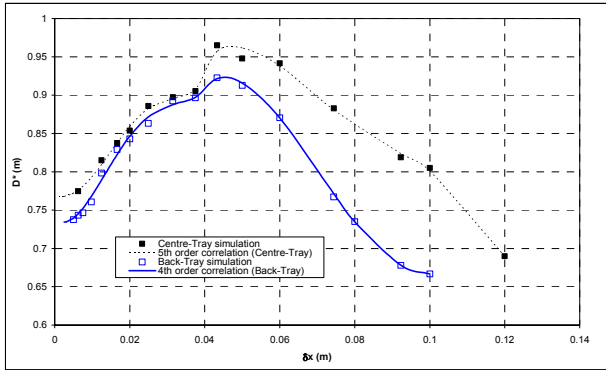


Figure 6. Characteristic fire diameter vs. nominal cell size profile.

Using the correlations shown in Fig.6,  $D^*$  (correlation) values and corresponding HRR ( $= D^{*5/2} \rho_{\infty} c_p T_{\infty} \sqrt{g}$ ) values have been calculated for various cell sizes. These HRR (correlation) values have been normalized by the grid-independent HRR (correlation) values for these fire scenarios. The normalized values represent a non-dimensional HRR with respect to a grid independent HRR value and are plotted against the non-dimensional quantity  $D^*/\Delta X$  in Fig.7. The result of similar analysis for 80 seconds was found to be almost identical, confirming the sufficiency of a selection of one-tenth duration of burnout time. Fig.7 represents a relationship between two non-dimensional quantities which is found very similar for the cases simulated in this study. Although this profile is unlikely to be universal, it may be worth to simulate different compartment fires to test this possibility.

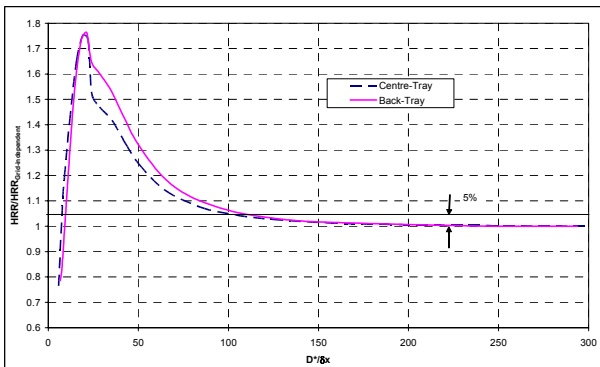


Figure 7. Normalized HRR versus  $D^*/\Delta X$  Profile

If the simulations were not conducted with the cell size  $< 35$  mm, the maxima of the profiles in Fig.6 and 7 could be mistakenly interpreted as the grid convergence. It appears that any result using  $D^*/\Delta X < 20$ , should be considered with extreme caution. Preliminary investigation shows that Eq.7 is responsible for the presence of these maxima. Fig.7 shows that to obtain a 5% accurate result with respect to a grid-independent result  $D^*/\Delta X$ , based on the average HRR, should be  $\approx 105$ . Interestingly enough, for the Back-Tray case based on Fig.7 we may obtain an identical HRR profile using cell sizes of 75 and 9.375 mm corresponding to the  $D^*/\Delta X$  values of 10 and 78, respectively. The results from two simulations and the experiment are compared in Fig.8. The

profiles from two simulations are different from the experimental data. However the overall agreement between the experimental and numerical profiles is much better than that observed in [6]. FDS4 has the limitation of not taking into account the container rim effect as well as heat transfer to the steel tray for liquid fuel.

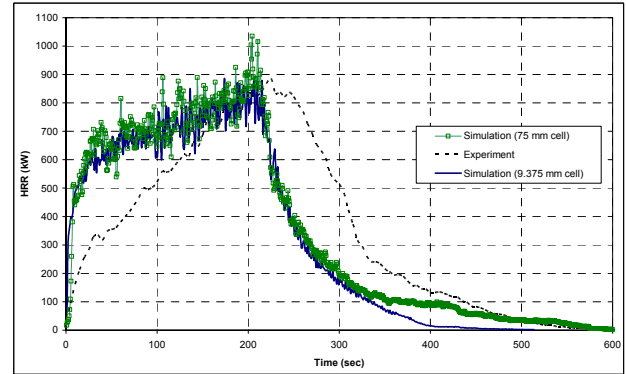


Figure 8. Comparison of HRR profiles obtained experimentally and from FDS simulation using 75 and 9.375 mm grid spacing.

## Conclusions

In this study to obtain grid independent results of a simple fuel package (liquid) fire in an ISO 9705 room, the required size of the computational cells have been evaluated using FDS4 model. It has been found that as the grid size decreases initially, the size of the fire increases then begins to decrease as the grid size decreases further. An analysis of the numerical data has been carried out to quantify this changing trend of fire size with respect to grid size. The analysis yielded a relationship (profile) between two non-dimensional quantities: HRR obtained using any grid/ grid independent HRR versus  $D^*/\Delta X$ . Preliminary study shows that Eq.7 is responsible for the presence of the maxima in this profile. Although this profile is unlikely to be universal, it is intended that further studies be undertaken to simulate different compartment fires to test the universality of this profile as it represents a relationship between two non-dimensional quantities. This profile will provide fire safety engineers an insight to make interpretations of their compartment fire simulation results obtained using computationally viable grids.

## Acknowledgments

This project was supported by VPAC e-Research Program Grant Scheme.

## References

- [1] McGrattan KB, Forney GP, Fire Dynamics Simulator (Version 4) User's Guide NIST Special Publication 1019, National Institute of Standards and Technology, U.S. Department of Commerce, Gaithersburg, MD, March 2006.
- [2] McGrattan KB (Ed.), Fire Dynamics Simulator (Version 4) Technical Guide NIST Special Publication 1018, National Institute of Standards and Technology, U.S. Department of Commerce, Gaithersburg, MD, March 2006.
- [3] Huggett C. Estimation of Rate of Heat Release by Means of Oxygen Consumption Measurements. Fire and Materials, 1980; 4: 61-65.
- [4] Moghaddam AZ, Moinuddin KAM, Thomas IR, Bennetts ID, Culton M. Fire Behaviour Studies of Combustible Wall Linings Applying FDS. Proceedings of 15th Australasian Fluid Mechanics Conference, Sydney, 2004.
- [5] Zou, GW, Chow, WK. Evaluation of Field Model, Fire Dynamics Simulator, for a Specific Experimental Scenario. Journal of Fire Protection Engineers, 2005; 15: 77-92.
- [6] Thomas IR, Moinuddin KAM, Bennetts ID. The Effect of Fuel Quantity and Location in Small Enclosure Fires. Journal of Fire Protection Engineering, 2007; 17: 85-102.